JOURNAL OF VIROLOGY, Dec. 2001, p. 12370–12381 Vol. 75, No. 24
0022-538X/01/$04.00+0 DOI: 10.1128/JVI.75.24.12370–12381.2001

Identification of Sequences in Brome Mosaic Virus Replicase Protein 1a That Mediate Association with Endoplasmic Reticulum Membranes

JOHAN A. DEN BOON,[1] JIANBO CHEN,[1] AND PAUL AHLQUIST[1,2]*

Institute for Molecular Virology[1] and Howard Hughes Medical Institute,[2] University of Wisconsin–Madison, Madison, Wisconsin 53706

Received 23 May 2001/Accepted 6 September 2001

RNA replication of all positive-strand RNA viruses is closely associated with intracellular membranes. Brome mosaic virus (BMV) RNA replication occurs on the perinuclear region of the endoplasmic reticulum (ER), both in its natural plant host and in the yeast *Saccharomyces cerevisiae*. The only viral component in the BMV RNA replication complex that localizes independently to the ER is 1a, a multifunctional protein with an N-terminal RNA capping domain and a C-terminal helicase-like domain. The other viral replication components, the RNA polymerase-like protein 2a and the RNA template, depend on 1a for recruitment to the ER. We show here that, in membrane extracts, 1a is fully susceptible to proteolytic digestion in the absence of detergent and thus, a finding consistent with its roles in RNA replication, is wholly or predominantly on the cytoplasmic face of the ER with no detectable lumenal protrusions. Nevertheless, 1a association with membranes is resistant to high-salt and high-pH treatments that release most peripheral membrane proteins. Membrane flotation gradient analysis of 1a deletion variants and 1a segments fused to green fluorescent protein (GFP) showed that sequences in the N-terminal RNA capping module of 1a mediate membrane association. In particular, a region C-terminal to the core methyltransferase homology was sufficient for high-affinity ER membrane association. Confocal immunofluorescence microscopy showed that even though these determinants mediate ER localization, they fail to localize GFP to the narrow region of the perinuclear ER, where full-length 1a normally resides. Instead, they mediate a more globular or convoluted distribution of ER markers. Thus, additional sequences in 1a that are distinct from the primary membrane association determinants contribute to 1a's normal subcellular distribution, possibly through effects on 1a conformation, orientation, or multimerization on the membrane.

Positive-strand RNA virus RNA replication occurs in close association with intracellular membranes. To date, no exceptions have been described, suggesting a pivotal role for membranes in the formation and functioning of the viral RNA replication complex. Direct evidence for the importance of membranes in virus RNA replication has been obtained in a few cases (6, 33, 53). Different viruses utilize different types of membranes. Alphaviruses and rubella virus assemble their replication complexes on endosomal and lysosomal membranes (13, 27), picornaviruses such as poliovirus use modified endoplasmic reticulum (ER) (7, 45, 47), and perinuclear ER membranes are used by arteriviruses (38, 52).

Brome mosaic virus (BMV) has a tripartite genome. Genomic RNAs 1 and 2 encode the viral RNA replication proteins 1a and 2a, respectively, that share three conserved domains with the replicases of members of the alphavirus-like superfamily (1, 16). Genomic RNA 3 encodes protein 3a, which is necessary for cell-to-cell movement during infection but not for RNA replication. A second, 3′-proximal gene on RNA3 encodes the coat protein that packages progeny RNA. Translation of this gene is realized via the transcription of a subgenomic mRNA, RNA4.

* Corresponding author. Mailing address: Institute for Molecular Virology and Howard Hughes Medical Institute, University of Wisconsin—Madison, 1525 Linden Dr., Madison, WI 53706. Phone: (608) 263-5916. Fax: (608) 265-9214. E-mail: ahlquist@facstaff.wisc.edu.

BMV replicase protein 1a (109 kDa) has a modular organization. The N-terminal half of the protein has demonstrated guanine-7-methyltransferase and guanylyltranferase activities, necessary for capping of viral RNAs (2, 24). The C-terminal half has a helicase-like domain (18) that is essential for all forms of BMV RNA synthesis (26). This helicase domain is closely related to Semliki Forest virus (SFV) nonstructural protein 2 (nsP2), which has been shown to have helicase, ATPase, and GTPase activities (17, 41). The two enzymatic modules in 1a are separated by a short proline-rich sequence with little predicted secondary structure that may be a flexible spacer (Fig. 1A). It has been postulated that, like other known helicases, two or more 1a proteins can interact to act as multimers rather than monomers. Evidence for 1a-1a interactions has been obtained by two-hybrid analyses (35, 37).

Besides providing enzymatic functions for RNA replication, 1a is the primary viral determinant for the subcellular localization of the BMV RNA replication complex. 1a localizes to the perinuclear ER both in its natural plant host and in the yeast *Saccharomyces cerevisiae* (39, 40). BMV replication in yeast faithfully duplicates most if not all stages of infection observed in plants cells, up to and including assembly of progeny virions (25). By studying BMV replication in yeast it was shown that 1a localizes independently to the ER in the absence of any of the other viral factors (39). In contrast, the predicted RNA-dependent RNA polymerase 2a depends on 1a for recruitment to the site of replication. This recruitment of 2a is

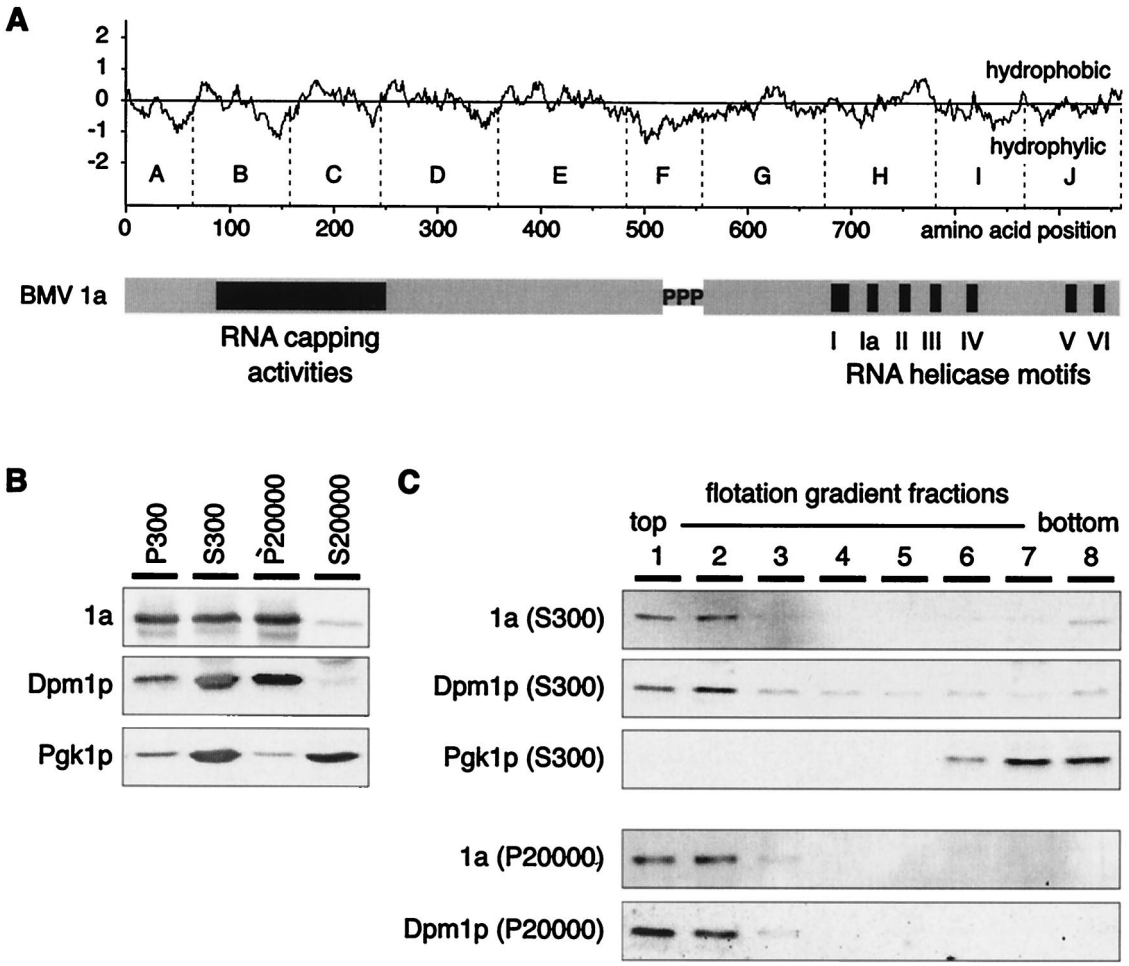

FIG. 1. (A) Schematic representation of BMV 1a with hydrophobicity plot. Shown is the modular organization of the 1a protein with the N-terminal RNA capping domain, the central proline-rich region, and the C-terminal DEAD box helicase-like domain. Highly conserved sequence elements are indicated in black. Hydrophobicity was calculated by using the algorithm of Hopp and Woods with a window size of 17 aa (19). The boundaries of regions referred to as A through J throughout the text have been indicated with dashed vertical lines. (B) Western blots showing subcellular fractionation of yeast cell lysates by differential centrifugation. Lysates were centrifuged at 300 × *g*, and the supernatant fraction, S300, was centrifuged at 20,000 × *g* to separate insoluble proteins from soluble proteins in P20,000 and S20,000 fractions, respectively. (C) Western blots showing flotation gradient profiles of subcellular fractions shown in panel B. The bottom three fractions represent the original sample loading volume. The profiles of cytosolic Pgk1p and integral ER membrane protein Dpm1p are shown as controls. The profile of Pgk1p from the P20,000 fraction is not shown since the low residual amount of Pgk1p in this fraction was below detection limits in the gradient fractions.

based on a well-documented direct interaction between the N terminus of 2a and the C terminus of 1a (23, 35, 36) and is reflected in a 1a-induced increase of 2a accumulation (9, 20). 1a also recruits viral RNA templates into replication, resulting in dramatically increased RNA stability but reduced translatability (21, 49). For both BMV RNA2 and RNA3, responsiveness to these 1a actions depends on defined *cis*-acting signals centered around a conserved motif matching the conserved sequence and structure of TΨC loops in tRNA (6a, 9, 48, 49).

The additional dependence of BMV RNA replication on multiple host functions is evident from the isolation of yeast strains with chromosomal mutations that interfere with BMV replication (11, 20, 34). Among these mutations is one in the OLE 1 locus that encodes for Δ9 fatty acid desaturase. The mutation results in a reduction of unsaturated fatty acid levels which has a direct effect on intracellular membrane composition. BMV replication in this mutant is severely reduced at a step between RNA template recruitment and negative-strand RNA synthesis, emphasizing the importance of compatibility of the membrane composition with RNA replication (32).

We have further examined the nature and determinants of BMV 1a-membrane association in yeast. This report describes our characterization of 1a's membrane topology, biochemical analyses of its membrane affinity, mapping of 1a sequences that control membrane association, and variations in subcellular localization patterns of green fluorescent protein (GFP)-tagged 1a deletion derivatives.

MATERIALS AND METHODS

Yeast cell culture and transformation. Yeast strain YPH500 (*MATα, ura3-52, lys2-801, ade2-101, trp1-Δ63, his3-Δ200, leu2-Δ1*) was used in all experiments. DNA transformation was carried out according to Gietz et al. (15). Cultures were

grown at 30°C in synthetic minimal medium containing 2% galactose. Medium lacked uracil and/or histidine to select for maintainance of DNA plasmids.

Plasmids. Plasmid pB1CT19 was used to express wild-type (wt) BMV 1a as described previously (22). Plasmid pA-59 DNA for expression of EMP47 with and N-terminal c-*myc* tag was kindly provided by Sean Munro (46). HIS3-selectable yeast 2μ plasmids expressing 1a or 1a deletion derivatives under control of the yeast ADH1 promoter were constructed by using standard recombinant DNA procedures (44). For deletion analysis, the 1a protein sequence was subdivided into regions A through J as shown in Fig. 1, 4, and 5, chosen not to disrupt regions of predicted hydrophobicity or secondary structure. Amino acid (aa) coordinates for these regions are as follows: A(1–68), B(69–158), C(159–247), D(248–366), E(367–480), F(481–557), G(558–676), H(677–782), I(783–867), and J(868–961). To generate the plasmids shown in Fig. 4 and 5, DNA fragments spanning the coding sequence for one or more of these regions were cloned as *Nco*I-*Eco*RI cassettes that were generated by PCR. Upstream oligonucleotide primers contained the sequence 5′-CC ATG GAC-3′ to introduce an *Nco*I restriction enzyme recognition site at the translation initiation codon, followed by a glycine codon immediately preceding the authentic BMV 1a sequence. At the downstream ends of the PCR fragments, *Eco*RI sites were introduced to generate termination codons by digestion with *Eco*RI, filling in of the 5′ overhangs by using T4 DNA polymerase in the presence of all four nucleotides, and subsequent religation. Alternatively, the *Eco*RI sites were used for in-frame fusion with the GFP gene. Plasmid yEGFP1 was used as the source of a version of GFP that is optimized for yeast codon usage (10). Plasmids that expressed 1a-derivatives with internal deletions were generated by inserting *Nco*I-*Nco*I PCR cassettes corresponding to the regions upstream of the intended deletion into the *Nco*I site of appropriate constructs that already contained the regions downstream from the deletion. All DNA fragments that were generated via PCR were analyzed by automated DNA sequencing at the facilities of the Biotechnology Center at the University of Wisconsin–Madison.

Subcellular fractionation. Yeast cells were grown to mid-logarithmic phase, i.e., to an optical density of 600 nm (OD_{600}) between 0.4 and 0.7. Ten OD_{600} units of cells were spheroplasted as described previously (43) and lysed in 200 μl of yeast lysis buffer (50 mM Tris-HCl, pH 7.7; 2.5 mM EDTA; 2.5 mM EGTA; 1 mM phenylmethylsulfonyl fluoride; 5 μg of pepstatin, 10 μg of leupeptin, and 10 μg of aprotinin per ml; 10 mM benzamidine) by vortexing the cells for 30 s with 200-μl glass beads. Lysates were centrifuged in a microcentrifuge for 2.5 min at 300 × *g* to pellet unbroken cells and incompletely disrupted cell debris (P300). The 300 × *g* supernatant (S300) was subsequently centrifuged at 20,000 × *g* to separate cytosolic and membrane-associated proteins in an S20,000 supernatant fraction and a P20,000 pellet fraction, respectively. Pellets were resuspended in lysis buffer and aliquots corresponding to equal OD_{600} units of the original cell culture were analyzed by standard sodium dodecyl sulfate-polyacrylamide gel electrophoresis (SDS-PAGE) and Western blotting procedures as described previously (2, 30).

Sucrose flotation gradient analysis. For flotation analysis, samples were adjusted to 52% (wt/wt) sucrose in lysis buffer, and 400 μl was loaded on the bottom of thick-walled polycarbonate TLS55 ultracentrifuge tubes (Beckman catalog no. 343778), overlaid with 900 μl of 45% sucrose in lysis buffer, topped with 100 μl of 10% sucrose in lysis buffer, and subsequently centrifuged at 40,000 rpm at 4°C for >16 h by using a TLS55 rotor in a Beckman Optima TLX tabletop ultracentrifuge. Gradients were manually fractionated in eight fractions of 175 μl, which were diluted with 300 μl of lysis buffer. Then, 10 μl of each diluted fraction was analyzed by SDS-PAGE and Western blotting procedures as described previously (2, 30).

Protease susceptibility assays. P20,000 subcellular fractions were prepared as described above but with the HEPES-based lysis buffer described by Feldheim et al. to prevent permeabilization of membrane compartments (12). No protease inhibitors were included during the procedure. The P20,000 was resuspended in 150 μl of Feldheim's lysis buffer, and 15-μl aliquots were added to 15 μl of 2× assay mixtures to achieve final concentrations of 0, 4, 8, 16, or 32 μg of proteinase K/ml in the presence or absence of 0.1% Triton X-100, and assays were incubated for 5 min on ice. Proteolytic activity was stopped by adding 15 μl of 3× SDS-PAGE loading buffer and immediately boiling for 10 min. Samples were analyzed by SDS-PAGE and subsequent Western blotting as described before (2, 30).

Membrane protein extraction analysis. P20,000 subcellular fractions were prepared from 20 OD_{600} units of yeast cells that were lysed by using the Tris-based lysis buffer described above. The final P20,000 fraction was resuspended in 350 μl of lysis buffer, and 70-μl aliquots either were kept at the same buffer conditions, or adjusted to 1 M NaCl or 100 mM Na_2CO_3 at a final pH of 11.5 or to 0.5% Triton X-100 in final volumes of 140 μl. The samples were then incubated for 30 min on ice, with brief vortexing 10 and 20 min into the incubation. Samples were adjusted to 52% sucrose in lysis buffer while maintaining the extraction conditions and analyzed on flotation gradients as described above.

Microscopy. Live cell imaging and confocal immunofluorescence microscopy were carried out as described previously using the confocal microscope facilties of the Keck neural imaging lab at the University of Wisconsin medical school (8, 39).

Antisera. Rabbit polyclonal antisera directed against BMV 1a and their use in Western blot analyses have been described elsewhere (40). Rabbit polyclonal anti-GFP antiserum and mouse monoclonal anti-Dpm1p and anti-Pgk1p antisera were purchased from Molecular Probes and were used at 1:6,000, 1:2,000, and 1:6,000 dilutions, respectively; rabbit polyclonal anti-Kar2p antiserum was provided by Mark Rose (42) and used at 1:1,000 or 1:500 for Western blotting and immunofluorescence analysis, respectively. Mouse monoclonal anti c-myc antiserum was purchased from Boehringer Mannheim and used at a 1:500 dilution for immunofluorescence analysis.

RESULTS

Flotation analysis of 1a-membrane association. Prior experiments have used differential centrifugation to investigate the membrane association of BMV 1a and BMV replication complexes in yeast and other cells (8, 9). However, a finding consistent with the hypothesis that 1a acts in a multimeric fashion, our initial experiments, and further results below indicated that 1a has a tendency to aggregate under certain buffer conditions. This complicates the interpretation of results based on sedimentation only, since under some conditions significant amounts of 1a can pellet even when not associated with membranes. Therefore, we included a subcellular fractionation protocol based on membrane flotation analysis to distinguish proteins in low-density membrane fractions from those in high-density protein aggregates. Yeast cells expressing 1a from a DNA plasmid were lysed and slow-speed centrifugation at 300 × *g* was used to pellet unbroken and incompletely disrupted cells. The resulting clarified lysate (S300) was centrifuged at 20,000 × *g* to sediment membranes and their associated proteins (Fig. 1B). As controls for the procedure, the integral ER membrane protein dolichyl-phosphate β-D-mannosyltransferase (Dpm1p) and the cytosolic protein phosphoglycerate kinase (Pgk1p) were analyzed in parallel. As expected, Dpm1p segregated with the P20,000 fraction, whereas Pgk1p was predominantly recovered in the S20,000 fraction. The 1a protein fractionated like Dpm1p, and to prove that this reflected true membrane association rather than aggregation the S300 and the P20,000 fractions were subjected to sucrose gradient flotation analysis. Lysate fractions were adjusted to 52% sucrose, loaded into the bottom of a centrifuge tube, overlaid with sucrose solutions of 45 and 10% sucrose, and centrifuged at 100,000 × *g* (see Materials and Methods). Using this approach, we found that membranes and membrane-associated proteins such as Dpm1p float up to reach equilibrium in the top fractions of the gradient (Fig. 1C). Cytosolic proteins such as Pgk1p remain at their original loading position in the three bottom fractions of the gradient (Fig. 1C). Most of the 1a in the S300 fraction and all of the 1a in the P20,000 fraction floated to the top of the gradient and were therefore membrane associated.

Protease susceptibility of membrane-associated 1a. Analysis of the primary sequence of 1a does not reveal clues to the basis of 1a association with the membrane. In particular, the hydrophobicity profile of 1a does not show any regions of sufficient length and hydrophobicity that could qualify as transmembrane regions (Fig. 1A). To investigate the distribution of 1a

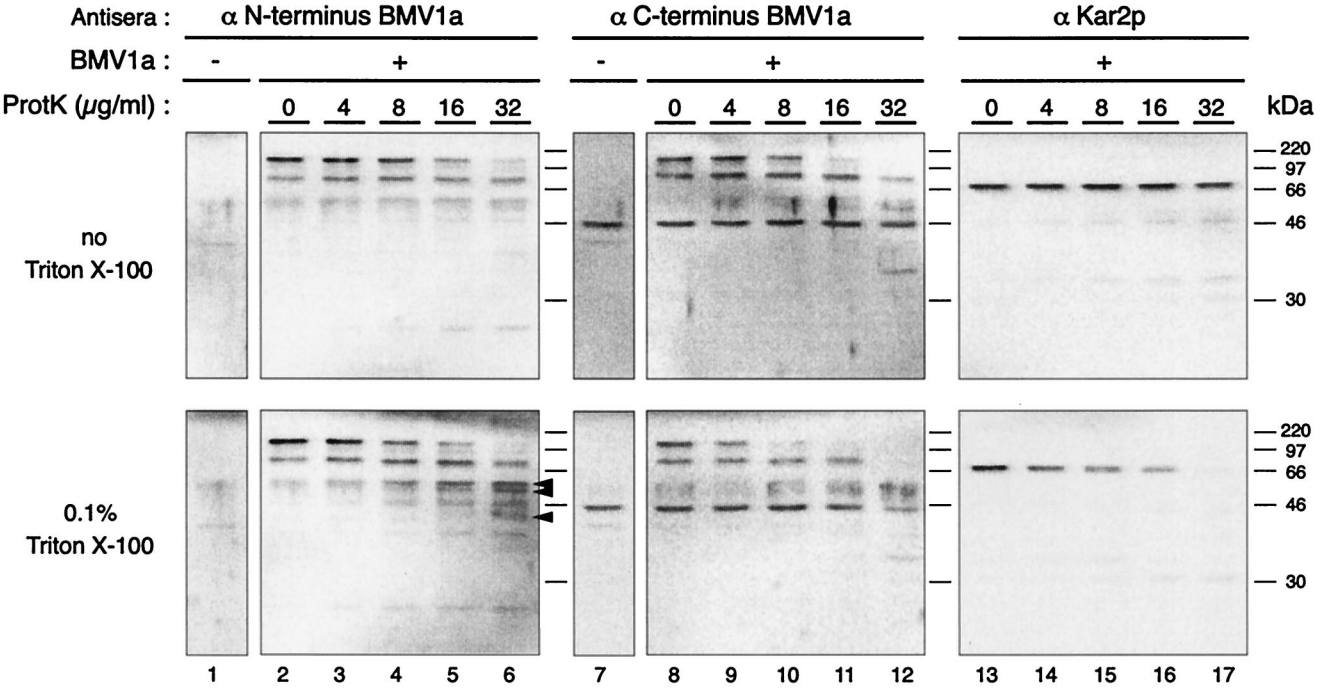

FIG. 2. Protease susceptibility of BMV 1a. Aliquots of P20,000 fractions of yeast cells expressing 1a or of control cells were incubated with increasing amounts of proteinase K. Assays were carried out in the absence (top panel) or presence (bottom panel) of 0.1% Triton X-100. For each sample, three separate Western blots are shown: one generated by using a mixture of two polyclonal antisera raised against either the N-terminal half of 1a, a second generated by using a mixture of two polyclonal antisera raised against the C-terminal half of 1a, and a third generated by using antiserum against yeast ER lumenal protein Kar2p as a control. Three solid arrowheads indicate the position of moderately resistant 1a-derived fragments in the presence of Triton X-100.

sequences with respect to the cytolosic and lumenal faces of the ER membrane, we assayed the susceptibility of 1a to proteolysis. We reasoned that parts of 1a that localize to the cytoplasmic face of the ER will be accessible for protease in a detergent-independent fashion, while any parts of 1a that protrude into the ER lumen should only be degradable after solubilization of the ER membrane with detergent. P20,000 membrane fractions were prepared from 1a-expressing yeast and subjected to increasing amounts of proteinase K (Fig. 2). As a control, Kar2p, a yeast ER lumenal protein homologous to mammalian BiP (42), was protected from proteolytic activity in the absence of detergent. The addition of Triton X-100 rendered Kar2p susceptible to degradation even at the lowest protease concentrations. A weakly visible, ca. 30-kDa band that cross-reacted with antiserum against Kar2p showed a degree of protease resistance that was independent of the presence or absence of Triton X-100 and therefore not due to membrane protection.

In parallel to that of Kar2p, the sensitivity of 1a to proteinase K was analyzed. One set of blots (Fig. 2, left panels) was probed with a mixture of two polyclonal antisera against the N-terminal half of 1a, while a second set of blots (Fig. 2, center panels) was probed with a mixture of two polyclonal antisera against the C-terminal half of 1a. Each set of antisera cross-reacted with protease-resistant fragments that were not 1a derived since they were also present in preparations from cells that did not express 1a (lanes 1 and 7). The anti-C-terminal antisera in particular showed high affinity for a 46-kDa protein (lanes 7 to 12). In contrast to Kar2p, 1a was equally susceptible to proteolysis in the absence or presence of Triton X-100. Degradation intermediates that accumulated and were degraded in a precursor-product relationship were observed, but none of these had increased susceptibility to protease upon addition of Triton X-100. In fact, the N-terminal 1a antisera detected three protease-resistant 1a-derived fragments of ca. 54, 52, and 44 kDa that were more protease resistant in the presence of Triton X-100 than in the absence of the detergent (see arrowheads, lane 6). Such increased protease resistance in the presence of detergent may result from 1a aggregation upon its release from membranes, as described further below. As for all such experiments that rely on immunological detection methods, our results do not rule out that there could be one or more lumenal regions of 1a that lack epitopes for the multiple, polyclonal anti-1a antisera used. Nevertheless, they show that substantial portions of both the N- and C-terminal halves of 1a are protease accessible, indicating that 1a is predominantly associated with the cytoplasmic face of the ER.

1a-membrane affinity. To gain more insight into the biochemical nature of the 1a-membrane association, we tested the ability of conditions of high ionic strength or high pH to release 1a from membranes in P20,000 fractions. These conditions are often used to probe membrane-protein affinity since they do not release integral membrane proteins with membrane-spanning domains but can release peripheral membrane proteins due to disruption of electrostatic protein-protein or protein-lipid interactions. High pH converts closed membrane vesicles to open membrane sheets, thereby releasing proteins and peripheral membrane proteins loosely associated with the in-

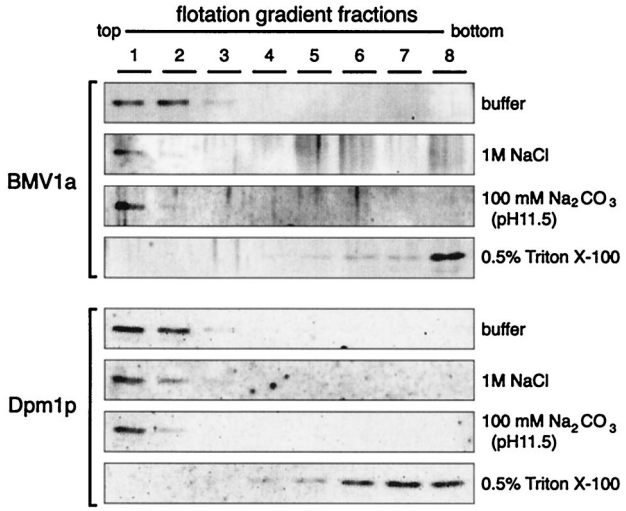

FIG. 3. Western blots showing flotation gradient profiles of BMV 1a and integral ER membrane protein Dpm1p from P20,000 fractions from yeast cells expressing 1a. Samples were floated after incubation for 30 min at 4°C under neutral, high-salt, high-pH, or detergent extraction conditions.

tralumenal membrane face (14). As a control, an additional sample of the membrane fraction was extracted with Triton X-100. All samples were analyzed by sucrose gradient flotation to distinguish between membrane association and aggregation, and the distribution of 1a in the gradients was compared to that of integral ER membrane protein Dpm1p. (Fig. 3). As expected, Dpm1p was not released from the membrane fraction by high salt or high pH but was released by Triton X-100. Similar to Dpm1p, 1a retained membrane association in high salt or high pH. Thus, despite the absence of obvious membrane-spanning segments, 1a displayed high affinity for membranes. The only difference between the behaviors of 1a and Dpm1p was seen in Triton X-100. Under these conditions, Dpm1p remained distributed through the bottom three gradient fractions, corresponding to the original sample loading volume. In contrast, in Triton X-100 1a collected exclusively in the bottom fraction of the gradient, a finding consistent with aggregation or multimerization.

Deletion analysis of 1a-membrane association. To assess the contribution of different sequences in 1a to membrane association, we carried out a deletion analysis. Plasmids were constructed that expressed 1a derivatives with C-terminal or the N-terminal truncations of various lengths or with internal deletions within the N-terminal half of 1a (Fig. 4A). The deletion endpoints were designed to divide 1a into segments A to J without disrupting predicted stretches of moderately hydrophobic sequence, α-helices or β-sheets. For each 1a deletion plasmid, two or more yeast cultures that were independently transformed were harvested, and the S300 were analyzed by sucrose gradient flotation. Relevant regions of representative Western blots are shown in Fig. 4B. Flotation efficiency was expressed as the percentage of total 1a or 1a-derived protein in the gradient that was present in the top three fractions.

In such assays, the flotation efficiency of wt 1a was 81 to 86% (Fig. 4B). This reflects that, while nearly all of the1a recovered in the P20,000 fraction floated with high membrane affinity [Fig. 1C, 1a (P20000), and Fig. 3], the S300 clarified lysate contained a small amount of 1a that neither pelleted at 20,000 × *g* (Fig. 1B) nor floated in a sucrose gradient [Fig. 1C, 1a (S300)] and thus may not have been membrane associated under the conditions used (see Discussion). Deleting C-terminal regions H to J did not alter the efficiency of 1a membrane association. When regions G or FG were deleted in addition, membrane flotation was reduced, but only to 25 to 42%. In contrast, most deletions in the N-terminal half of 1a reduced membrane association to near background levels. Only two deletions in the N-terminal domain retained significant membrane association: deleting segment A yielded a flotation efficiency of ca. 30%, while deleting A to C resulted in ca. 60 to 70% flotation. All other deletions, including deleting segments B, C, D, E, and F individually, reduced membrane association to ca. 10% or less. Although D-J had retained high levels of membrane association, when combined with region AB in construct ΔC, flotation was no longer apparent. Also, the addition of regions G to J reduced membrane association of regions A to E (ΔF, Fig. 4).

Together, these results show that 1a membrane association was more strongly affected by N-proximal than C-proximal deletions and that 1a contains sequences with high membrane affinity outside of regions A to C and H to J, but that the function of these regions depends on the surrounding protein context.

1a subdomains target GFP to the membrane. To determine whether the sequences that proved to be important for 1a-membrane association in deletion variants were also sufficient to direct membrane association, we carried out a gain-of-function analysis. We fused GFP to selected 1a domains and tested for segregation of the hybrid proteins with the membrane fraction in flotation gradients (Fig. 5). Since deletion of 1a segments H, I, and J did not interfere with membrane association (Fig. 4), the analysis was restricted to segments A through G. To increase the chance that at least some fusions would contain an intact membrane-association domain, three series of overlapping 1a-GFP fusions were made in which three consecutive, two consecutive, or single 1a segments from region A-G were fused to the GFP N terminus (Fig. 5A). The results of flotation analyses with these fusion proteins are shown in Fig. 5B.

The highest flotation efficiency, 60 to 66%, was seen with DE-GFP. Further dissection of the DE region showed that E-GFP retained 27 to 29% flotation efficiency, while the flotation of D-GFP was near background levels. Interestingly, regions C and F adversely affected flotation, reducing flotation efficiency from ~63% for DE-GFP to ~33% for CDE- and DEF-GFP. Fusions that lacked 1a region E generally showed little or no membrane association above background levels. Of these, the most significant flotation, ~20%, was found for AB-GFP. However, results below show that the intracellular localization of AB-GFP was distinct from that of wt 1a and DE-containing fusions. Addition of region C to AB-GFP again interfered with flotation, reducing the flotation of ABC-GFP to near-background levels.

Since both the deletion analyses and the gain-of-function analyses showed that 1a region DE and E had significant effects on membrane targeting, we explored whether the affinity of the membrane association conferred by in particular region DE was as high as that of wt 1a. As shown in Fig. 6, P20,000

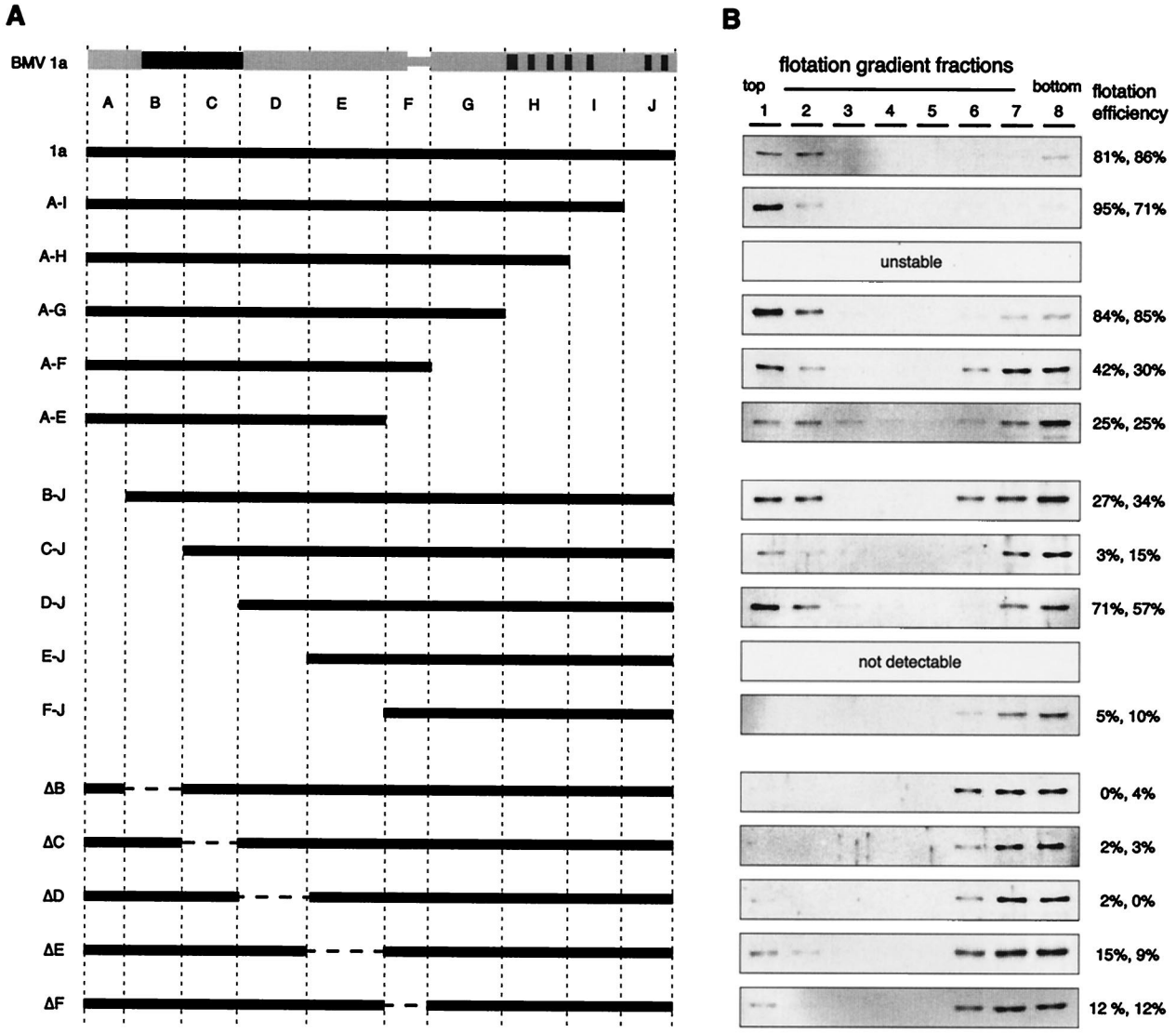

FIG. 4. Deletion mapping of 1a membrane association domains. (A) Diagram of 1a deletion constructs designed on the basis of a subdivision of 1a into 10 regions, A through J (Fig. 1A), chosen such that elements of predicted hydrophobicity and/or secondary structure were left intact. (B) Western blots showing flotation gradient profiles for each of the 1a deletion derivatives and corresponding flotation efficiencies, expressed as the percentage of total protein that was present in the top three fractions of the gradient. All analyses were done in duplicate by using two independent yeast transformants, and representative results are shown. Western blots were exposed for different lengths of time to approximate equal signal intensities. The gradient profile of protein A-H was omitted because this protein was found to accumulate in degraded fragments, preventing determination of the behavior of the full-length protein. Protein E-J could not be detected.

membrane fractions from cells expressing DE-GFP, E-GFP, and wt 1a were treated with high salt, high pH, or Triton X-100, and analyzed by flotation gradients to compare the effects on membrane association. To allow visualization of the multimeric characteristics of 1a or the formation of high-density 1a aggregates, the membrane extracts were loaded on top of a 65% sucrose cushion added to the bottom of each gradient. As controls, we monitored the effects of each treatment on the overall spectrum of yeast proteins in these membrane fractions and on integral ER membrane protein Dpm1p by using total protein staining and Western blotting, respectively. Total protein staining showed that, in the standard extraction buffer, most proteins in the P20,000 fraction floated to the top of the gradient with membranes, while the 1 M NaCl and pH 11.5 treatments each caused significant fractions of these proteins to remain in the lower part of the gradient (Fig. 6, top panels). Nevertheless, as in Fig. 3, integral ER protein Dpm1p and 1a remained membrane associated under both conditions (Fig. 6, lower panels). As expected, Triton X-100 prevented all membrane proteins, including Dpm1p and 1a, from floating. In this detergent, most proteins including Dpm1p remained primarily in the 52% sucrose layer in which the sample was originally loaded (gradient fractions 5 and 6). In contrast, in Triton X-100, 1a primarily sedimented into the top of the 65% sucrose cushion at the bottom of the gradient (fractions 7 and 8). Thus, after being released from the membrane, 1a may either be associated in higher order protein structures or aggregate through hydrophobic regions or other contacts (see Discussion).

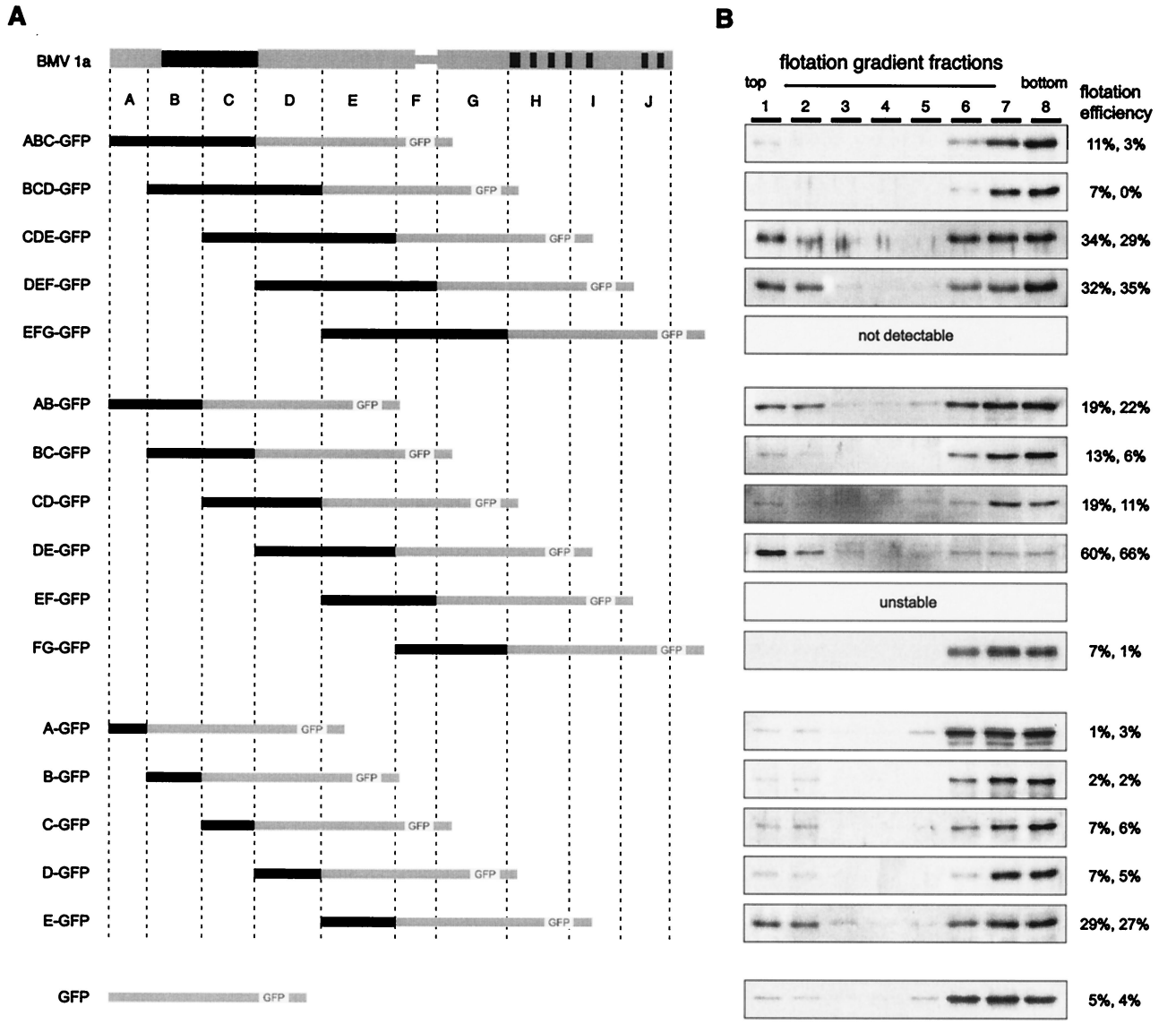

FIG. 5. Gain-of-function analysis for membrane association by using 1a derived sequences fused to GFP. (A) Diagram of 1a-GFP derivatives. (B) Western blots showing flotation gradient profiles for each of the 1a-GFP-derived fusion proteins and their corresponding flotation efficiencies calculated as in Fig. 4. The gradient profiles of EFG-GFP and EF-GFP were omitted because of poor detectability and instability, as indicated. The flotation behavior of free GFP is shown at the bottom as a control.

The strong affinity of 1a for membranes was largely retained in DE-GFP, which continued to float with membranes in 1 M NaCl and pH 11.5 (Fig. 6, lower panels). E-GFP also primarily floated under these conditions. As expected, in Triton X-100, DE-GFP, and E-GFP were dissociated from the membrane, but their distribution paralleled Dpm1p more closely than that of 1a. DE-GFP and E-GFP primarily localized to the 52% sucrose loading layer of the gradient (Fig. 6, right panels, fractions 5 and 6) rather than sedimenting into the 65% sucrose cushion (fractions 7 and 8).

Intracellular localization of 1a-GFP and deletion derivatives. Confocal microscopy shows that, in plant and yeast cells, wt 1a localizes to ER membranes, where it is retained without detectable accumulation in the Golgi or other later compartments of the secretory pathway (39, 40). To see whether the 1a sequences identified above to direct membrane association were sufficient to mediate the intracellular distribution of 1a, we used confocal fluorescence microscopy to examine cells expressing 1a-GFP fusions that retained significant membrane flotation efficiency. Kar2p was used as an ER marker (42), and nuclei were visualized by fluorescent staining of DNA. Numerous cells were examined for each 1a-GFP fusion protein, and representative examples are shown in Fig. 7. In all cases, the pattern of green fluorescence seen in live cells (leftmost panels) matched that seen in fixed cells (right panels). Free GFP was dispersed diffusely throughout the cell and showed no membrane association in cell fractionation (Fig. 5 and 7). In contrast, when GFP was fused to the C terminus of full-length

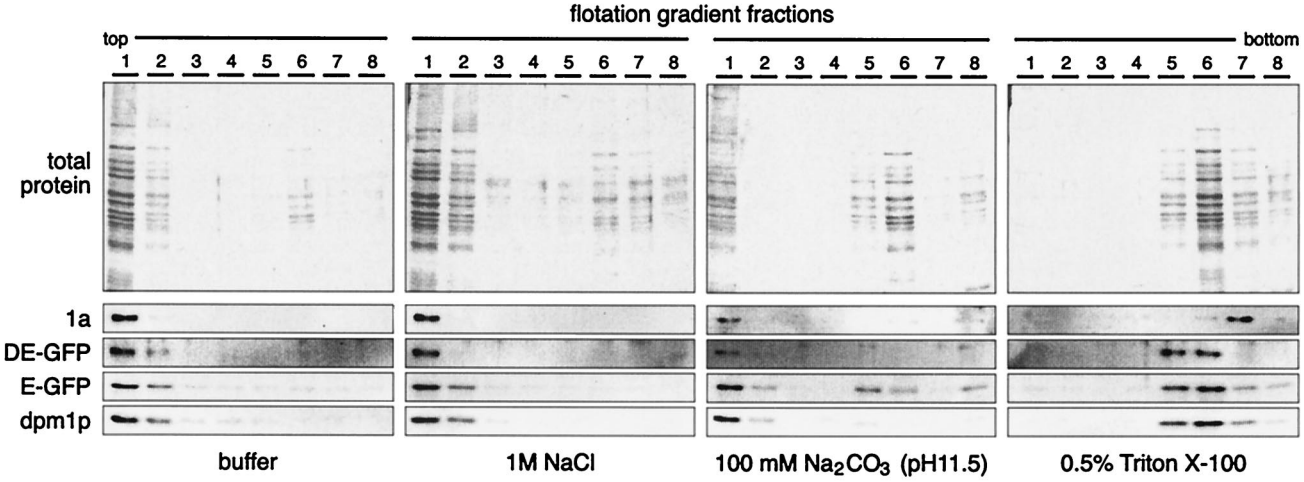

FIG. 6. Flotation gradient analysis of 1a, DE-GFP, and E-GFP from P20,000 fractions that were prepared from yeast cells as in Fig. 1 and incubated under neutral, high-salt, high-pH, or Triton X-100 extraction conditions prior to centrifugation. As a control, integral transmembrane protein Dpm1p was analyzed by using the same samples used to analyze 1a. The top panel shows Coomassie brilliant blue-stained gels identical to those used to generate the Western blots for 1a and Dpm1p shown immediately below.

1a, green fluorescence mirrored the distribution of wt 1a by colocalizing with the ER marker Kar2p, predominantly in the perinuclear region (Fig. 7, third row of images).

Similarly, the sites of CDE-GFP, DEF-GFP, and DE-GFP fluorescence also coincided with sites of Kar2p accumulation, again indicating ER localization (Fig. 7, rows 4 to 6). However, while 1a and 1a-GFP localized to the narrow perinuclear region of the ER, CDE-, DEF-, and DE-GFP accumulated in broader, more globular, or more convoluted structures that were often adjacent to the nucleus but not confined to the perinuclear region. Thus, it appeared that these fusion proteins caused rearrangement of the Kar2p signal. Sites of DEF-GFP accumulation in particular were bright spots or globules coinciding with denser accumulation of Kar2p signal than in neighboring portions of the ER. Interestingly, the sites of E-GFP fluorescence and some sites of DE-GFP fluorescence were adjacent to but only weakly and partially overlapping ER markers (Fig. 7, rows 6 and 7). The pattern of AB-GFP fluorescence, which localized in very bright spots, was distinct from that of other 1a-GFP fusions (Fig. 7, row 8). Usually, only a single spot was seen per cell, but the size of such spots frequently approached that of the nucleus. Moreover, unlike GFP fusions that contained 1a domain E and flanking regions, the AB-GFP fluorescent spots localized completely independently of the ER distribution.

Since E-GFP localized in spots closely adjacent to or partially overlapping the ER, we wanted to determine whether E-GFP might be passing into the Golgi apparatus, which in yeast normally appears as a series of spots that are often near the ER. Accordingly, we compared the localization of E-GFP and, as a control, 1a-GFP to that of c-myc tagged Emp47, a protein that resides in the Golgi apparatus (46). As shown in Fig. 8, neither 1a-GFP nor E-GFP showed any colocalization with the Golgi.

DISCUSSION

As outlined in the introduction, a universal feature of positive-strand RNA virus RNA replication is its association with intracellular membranes. In this study we used biochemical assays and microscopy to analyze multiple aspects of the membrane association of BMV RNA replication protein 1a, which targets the BMV RNA replication complex to the membrane. The combined data allow us to draw four main conclusions. First, 1a is localized to the cytoplasmic face of the ER. Second, minimal sequence determinants for membrane association of 1a are between aa 1 and 158 (region AB) and aa 367 and 480 (region E) in the N-terminal RNA capping domain. However, neither is sufficient to confer a wt level of 1a-membrane association, and region AB in particular fails to localize to the ER membrane. Third, a larger region, DE (aa 248 to 480), is both necessary and sufficient for high-affinity 1a-ER membrane association. Fourth, additional sequences in 1a outside of region DE contribute to maintain the normal subcellular distribution of wt 1a and ER markers.

1a-ER membrane topology and affinity. The results of our protease susceptibility analyses (Fig. 2) showed that 1a was largely, if not completely, accessible from the cytoplasm and that 1a was therefore predominantly on the cytoplasmic face of the ER with no detectable lumenal protrusions. This is consistent with an apparent lack of highly hydrophobic, potentially membrane-spanning sequences and, moreover, with the known roles of 1a in RNA replication. These roles include recruiting RNA templates from translation into replication (9, 21, 49), relocalizing the otherwise cytoplasmic 2a polymerase to the ER membrane (8, 35, 36, 39), and capping progeny viral RNA (2, 24) that is subsequently released into the cytoplasm to be translated or encapsidated.

Despite having a predicted peripheral membrane topology, in our membrane protein extraction assays, the majority (~85%) of wt 1a was associated with membranes with high affinity. Conditions of high salt or elevated pH that dissociate most other peripheral membrane proteins did not release1a from the membrane fraction (Fig. 3 and 6). Nevertheless, it is of interest that ~15% of wt 1a in S300 clarified lysates failed to pellet with membranes at 20,000 × *g* or to float with membranes in sucrose gradients (Fig. 1B, C). This smaller fraction

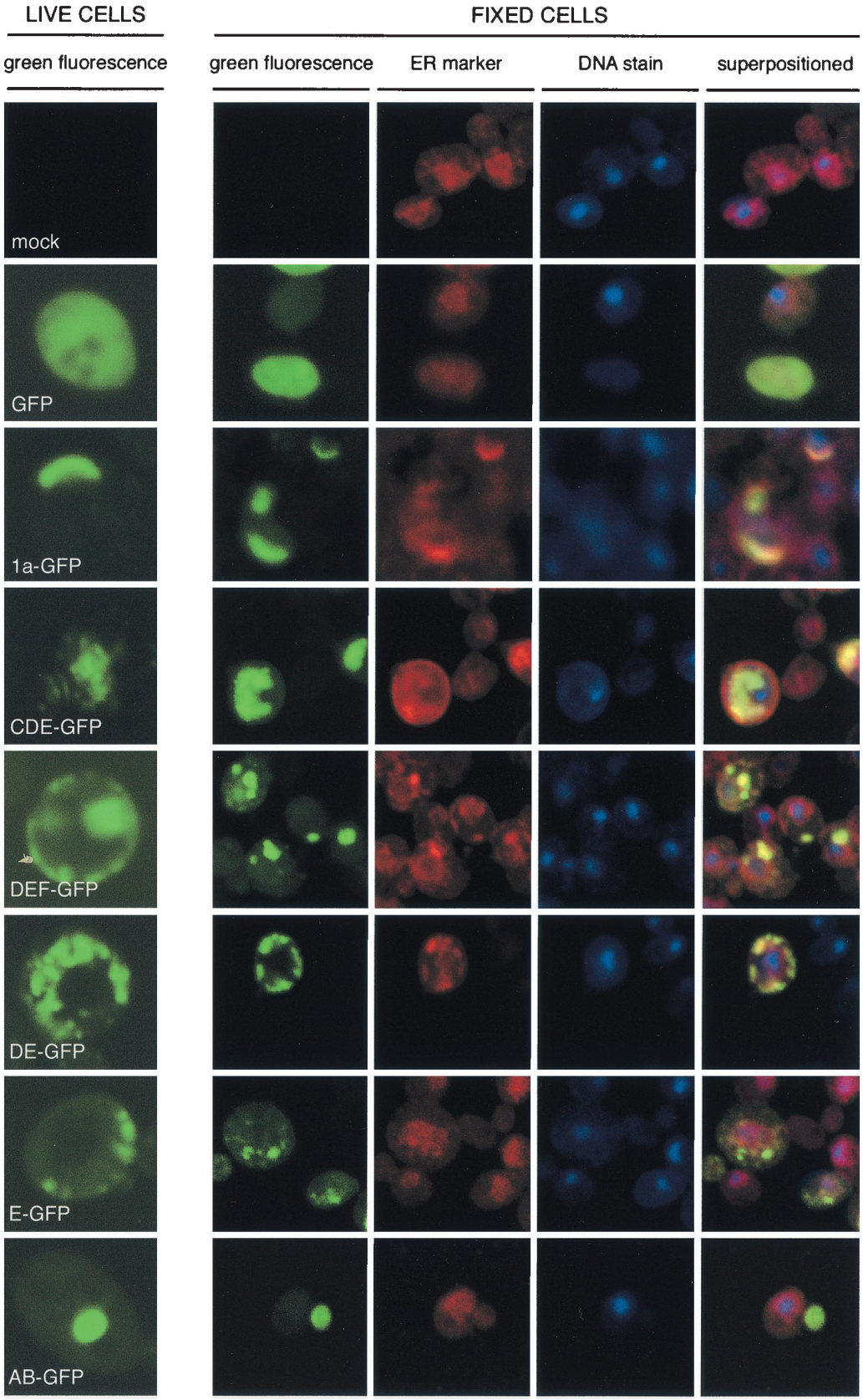

FIG. 7. Fluorescence microscopy analysis of mock-transformed yeast cells or yeast cells expressing GFP, 1a-GFP, and selected 1a-GFP deletion derivatives from Fig. 5 with significant membrane flotation efficiency. The left column shows representative green fluorescence images of live cells, displayed at twofold-higher magnification than the fixed cell images to the right. The four columns at the right show representative multichannel confocal fluorescence images of the corresponding formaldehyde-fixed cells. GFP was visualized by intrinsic fluorescence, ER was visualized by using anti Kar2p antiserum and Texas red-conjugated secondary antibodies, and DNA was stained by using TO-PRO-3 iodide.

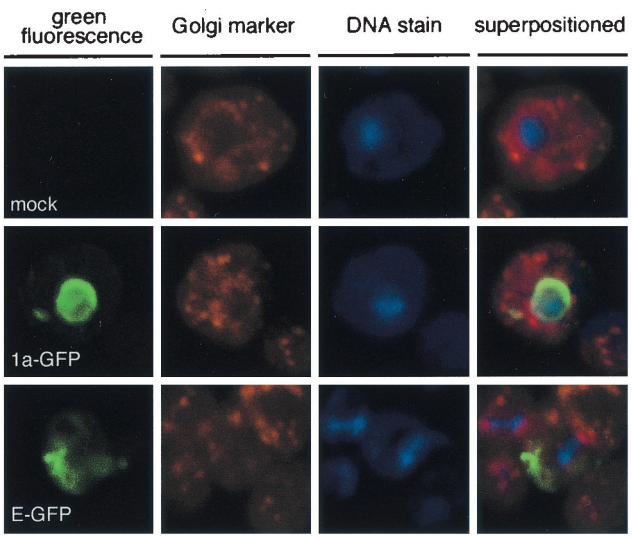

FIG. 8. Confocal microscopy analysis of formaldehyde-fixed cells mock transformed or yeast cells transformed with plasmids expressing 1a-GFP or E-GFP. The Golgi system was visualized by using anti-c-myc antiserum and Texas red-conjugated secondary antibodies to detect plasmid-expressed yeast Emp47-tagged N-terminally with a c-*myc* epitope. DNA was stained by using TO-PRO-3 iodide.

of 1a was either never membrane associated or more loosely associated and lost from the membrane fraction during the processing of the cell lysates prior to analysis. Since 1a lacks a classical signal sequence, it is not unlikely that its synthesis occurs on free ribosomes and that a small amount of 1a is therefore not immediately membrane bound, perhaps even fulfilling additional, as-yet-unidentified functions as a free cytoplasmic protein. The second alternative, losing a small fraction of loosely membrane-associated 1a, is consistent with a model in which 1a monomers interact peripherally with the membrane and in which self-interactions between multiple 1a monomers result in a higher-order protein structure with stronger membrane affinity characteristics. Two-hybrid results show that 1a has the potential for at least two self-interactions: intermolecular interactions between the N-terminal halves of two 1a proteins and intra- or intermolecular interactions between the N- and C-terminal halves (35, 37). Our observation that full-length 1a, when released from membranes by detergent treatment, sediments into 65% sucrose in the flotation gradients (Fig. 6) is an additional argument for the 1a-1a interaction model.

Experiments with 1a deletion derivatives and GFP fusions showed that sequences in the N-terminal RNA capping module of 1a were necessary and sufficient for the high-affinity of 1a-ER membrane association (Fig. 4 to 7). In particular, region DE between aa 248 and 480 largely retains the high affinity seen for full-length wt 1a. When separating regions D and E, the association with membranes, albeit with much-reduced efficiency, segregates with region E (Fig. 5). Partial dissociation of region E fused to GFP from membranes at pH 11.5 (Fig. 6) suggested that region E does not contain a membrane spanning sequence. This is consistent with the results of our limited proteolysis assays that showed that there is no evidence for protrusions of 1a into the ER lumen.

While 60 to 70% of 1a derivative D-J or DE-GFP was membrane associated, this membrane association was dramatically reduced by adding N-proximal 1a sequences (e.g., Fig. 4, derivative C-J, and Fig. 5, CDE-GFP). Similarly, 1a-membrane interaction was disrupted by deleting some segments that were not required for membrane association in other contexts (Fig. 4, ΔB and ΔC). Thus, the ability of 1a region DE or E to direct membrane association was highly sensitive to the context of surrounding 1a sequences. This high dependence of 1a-membrane interaction on protein context argues in favor of a membrane association model of higher complexity in which the accessibility and orientation of particular 1a domains for self interaction, interaction with host proteins or lipids is crucial.

Intracellular localization of 1a-GFP and deletion derivatives. In plant cells and yeast, wt 1a and BMV RNA replication complexes localize exclusively to ER membranes (39, 40), and we have shown here that 1a with a C-terminal GFP tag duplicates this distribution (Fig. 6). The degree of colocalization of 1a-GFP and its derivatives with ER markers correlated closely with their flotation behavior in the biochemical analyses. Full-length 1a had the highest flotation efficiency and 1a-GFP displayed complete colocalization with ER marker Kar2p. Association with the yeast ER was preserved by 1a deletion derivatives retaining region DE, including CDE-, DEF-, and DE-GFP (Fig. 7). However, while sufficient to direct ER membrane association, these 1a derivatives did not reproduce the normal cellular distribution of wt 1a-ER complexes. CDE- and DE-GFP localized in broader or more convoluted patterns, and DEF-GFP showed more globular distributions (Fig. 7). Colocalization of these structures with Kar2p implied that the ER membranes are rearranged by these fusion proteins. Similar abnormal membrane rearrangements, including globular masses of compactly folded membranes, are also induced by picornavirus membrane-associated RNA replication proteins 2C, 2BC or their deletion derivatives in the absence of other viral proteins (46, 50, 51). The ability of some BMV 1a fragments to alter the intracellular distribution of ER marker Kar2p is apparently controlled in full-length 1a by sequences outside the primary membrane association determinants. These sequences may function directly in additional types of membrane association, e.g., by interacting with host-encoded ER proteins or lipids, or by influencing 1a conformation or self-interaction. Thus, in some 1a fragments, improperly oriented or unregulated 1a-1a interaction may lead to aberrant 1a complexes and membrane rearrangements. Moreover, for some 1a fragments, aggregation might block interaction of some 1a monomers with membrane, explaining reduced membrane affinity. For such aggregates, possibly including CDE-GFP and DEF-GFP, mechanical disruption of such looser membrane association might result in gradient analysis results (Fig. 5) that underestimate the degree of in vivo membrane association (Fig. 7).

Membrane association of alphavirus-like replicases. From a virus evolution perspective, the BMV 1a-membrane association is consistent with its classification as an alphavirus-like virus. The results presented here reveal multiple parallels between membrane localization of RNA replication complexes by BMV and alphaviruses such as SFV. The N-terminal half of BMV 1a is the equivalent of alphavirus nsP1, the N-terminal cleavage product of the alphavirus replicase polyprotein. Like

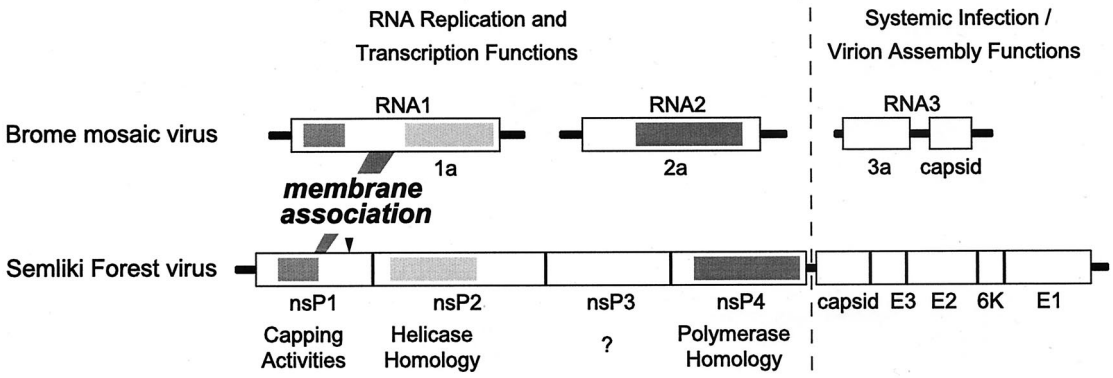

FIG. 9. Comparison of the genome organizations of BMV with that of alphavirus representative SFV. The evolutionary relationship within the superfamily of alphavirus-like viruses is based on regions of high amino acid conservation and is indicated with boxes of different shading. BMV 1a region E, located between aa 367 and 480, and the amphipatic helix, located between aa 245 and 264, in SFV nsP1 define the primary membrane association determinants. These regions do not share sequence homology but share similar positions downstream from the core homologies of the RNA capping domain. The location in SFV nsP1 of two palmitoylation sites in a stretch of three cysteines (aa 418 to 420), which are also implicated in membrane association, is indicated with a single black arrowhead.

BMV 1a, nsP1 contains the enzymatic guanine-7-methyltransferase and guanylyltranferase activities that are necessary for capping of the viral RNA (2, 3, 24, 29). Both proteins appear to lack segments with sufficient hydrophobicity to serve as membrane-spanning domains, but even so they remain associated with membranes under stringent extraction conditions such as high salt or high pH. Like BMV 1a, SFV nsP1 has a tendency to aggregate, suggesting self-interacting potential (29). Moreover, the membrane association determinant that we have now mapped in region E of BMV 1a is C terminal from the core sequences of the capping enzyme, in a similar position as one of two regions in (SFV) nsP1 that have been implicated in membrane association (Fig. 9). SFV nsP1 aa 245 to 264 form an amphipathic helix that interacts with negatively charged lipids by basic residues and a tryptophan residue that is inserted into the outer leaflet of the lipid bilayer (31). Palmitoylation of a second region in nsP1 at cysteines 418 to 420 enhances membrane affinity (4, 28). When palmitoylation is blocked, nsP1 is released from membranes by 1 M NaCl (4). Nevertheless, palmitoylation is dispensable for high-titer virus replication in vivo, including RNA replication on the normal membrane sites (4, 28).

Despite their similarities, BMV 1a and SFV nsP1 target different intracellular membranes, with BMV replication complexes assembling on ER membranes (39, 40), while alphavirus replication complexes assemble on endosomal and lysosomal membranes (13). Based on previously published sequence alignments, the region in BMV 1a that may correspond to the membrane-associating α-helix in SFV is in the N terminus of region D (2, 5). However, while it enhanced the intrinsic membrane association of segment E, segment D showed no membrane association capability, either on its own or in combination with more N-terminal 1a sequences (Fig. 4 and 5). The basis for the high affinity of 1a for membranes is not known. Among other factors, it might involve fatty acylation, formation of an amphipathic helix as in SFV nsP1, or interaction with host ER membrane proteins. The 1a N terminus lacks a myristoylation signal and attempts to label 1a with palmitate were unsuccessful (T. Ahola, unpublished results). On the other hand, region E does contain a long predicted α-helix of 32 aa that has several interesting characteristics. A helical wheel presentation of this region reveals a cluster of aromatic residues on one side of the helix that could have a function in membrane association similar to that of the tryptophan residue in SFV nsP1. On the opposite side of the helix is a cluster of positively charged residues that could mediate electrostatic interactions. Furthermore, a third clustering of leucines has the potential to facilitate the formation of a leucine zipper in a 1a-1a interaction model. Further experiments are needed to more precisely map the membrane association determinants and relevant flanking regions and to determine their mechanisms of action.

ACKNOWLEDGMENTS

We thank Lance Rodenkirch for excellent technical assistance with confocal microscopy using the facilities in the Keck Neural Imaging Laboratory of the University of Wisconsin-Madison. We also thank Becky Montgomery and members of our laboratory for stimulating discussions during the course of this work.

This research was supported by National Institutes of Health grant GM35072. P.A. is an investigator of the Howard Hughes Medical Institute.

REFERENCES

1. **Ahlquist, P., E. G. Strauss, C. M. Rice, J. H. Strauss, J. Haseloff, and D. Zimmern.** 1985. Sindbis virus proteins nsP1 and nsP2 contain homology to nonstructural proteins from several RNA plant viruses. J. Virol. **53:**536–542.
2. **Ahola, T., and P. Ahlquist.** 1999. Putative RNA capping activities encoded by brome mosaic virus: methylation and covalent binding of guanylate by replicase protein 1a. J. Virol. **73:**10061–10069.
3. **Ahola, T., and L. Kääriäinen.** 1995. Reaction in alphavirus mRNA capping: formation of a covalent complex of nonstructural protein nsP1 with 7-methyl-GMP. Proc. Natl. Acad. Sci. USA **92:**507–511.
4. **Ahola, T., P. Kujala, M. Tuittila, T. Blom, P. Laakkonen, A. Hinkkanen, and P. Auvinen.** 2000. Effects of palmitoylation of replicase protein nsP1 on alphavirus infection. J. Virol. **74:**6725–6733.
5. **Ahola, T., A. Lampio, P. Auvinen, and L. Kääriäinen.** 1999. Semliki Forest virus mRNA capping enzyme requires association with anionic membrane phospholipids for activity. EMBO J. **18:**3164–3172.
6. **Barton, D. J., and J. B. Flanegan.** 1993. Coupled translation and replication of poliovirus RNA in vitro: synthesis of functional 3D polymerase and infectious virus. J. Virol. **67:**822–831.

6a. **Baumstark, T., and P. Ahlquist.** The brome mosaic virus RNA3 intergenic replication enhancer folds to mimic a tRNA T ψC-stem loop and is modified in vivo. RNA, in press.

7. **Bienz, K., D. Egger, and L. Pasamontes.** 1987. Association of polioviral proteins of the P2 genomic region with the viral replication complex and virus-induced membrane synthesis as visualized by electron microscopic immunocytochemistry and autoradiography. Virology **160:**220–226.
8. **Chen, J., and P. Ahlquist.** 2000. Brome mosaic virus polymerase-like protein 2a is directed to the endoplasmic reticulum by helicase-like viral protein 1a. J. Virol. **74:**4310–4318.
9. **Chen, J., A. Noueiry, and P. Ahlquist.** 2001. Brome mosaic virus protein 1a recruits viral RNA2 to RNA replication through a 5′ proximal RNA2 signal. J. Virol. **75:**3207–3219.
10. **Cormack, B. P., G. Bertram, M. Egerton, N. A. R. Gow, S. Falkow, and A. J. P. Brown.** 1997. Yeast-enhanced green fluorescent protein (yEGFP)a reporter of gene expression in *Candida albicans*. Microbiology **143**(Pt. 2)**:** 303–311.
11. **Diez, J., M. Ishikawa, M. Kaido, and P. Ahlquist.** 2000. Identification and characterization of a host protein required for efficient template selection in viral RNA replication. Proc. Natl. Acad. Sci. USA **97:**3913–3918.
12. **Feldheim, D., J. Rothblatt, and R. Schekman.** 1992. Topology and functional domains of Sec63p, an endoplasmic reticulum membrane protein required for secretory protein translocation. Mol. Cell. Biol. **12:**3288–3296.
13. **Froshauer, S., J. Kartenbeck, and A. Helenius.** 1988. Alphavirus RNA replicase is located on the cytoplasmic surface of endosomes and lysosomes. J. Cell Biol. **107**(Pt. 1)**:**2075–2086.
14. **Fujiki, Y., A. L. Hubbard, S. Fowler, and P. B. Lazarow.** 1982. Isolation of intracellular membranes by means of sodium carbonate treatment: application to endoplasmic reticulum. J. Cell Biol. **93:**97–102.
15. **Gietz, D., A. St. Jean, R. A. Woods, and R. H. Schiestl.** 1992. Improved method for high efficiency transformation of intact yeast cells. Nucleic Acids Res. **20:**1425.
16. **Goldbach, R.** 1987. Genome similarities between plant and animal RNA viruses. Microbiol. Sci. **4:**197–202.
17. **Gomez de Cedron, M., N. Ehsani, M. L. Mikkola, J. A. Garcia, and L. Kaariainen.** 1999. RNA helicase activity of Semliki Forest virus replicase protein NSP2. FEBS Lett. **448:**19–22.
18. **Gorbalenya, A. E., E. V. Koonin, A. P. Donchenko, and V. M. Blinov.** 1988. A conserved NTP-motif in putative helicases. Nature **333:**22.
19. **Hopp, T. P., and K. R. Woods.** 1981. Prediction of protein antigenic determinants from amino acid sequences. Proc. Natl. Acad. Sci. USA **78:**3824–3828.
20. **Ishikawa, M., J. Diez, M. Restrepo-Hartwig, and P. Ahlquist.** 1997. Yeast mutations in multiple complementation groups inhibit brome mosaic virus RNA replication and transcription and perturb regulated expression of the viral polymerase-like gene. Proc. Natl. Acad. Sci. USA **94:**13810–13815.
21. **Janda, M., and P. Ahlquist.** 1998. Brome mosaic virus RNA replication protein 1a dramatically increases in vivo stability but not translation of viral genomic RNA3. Proc. Natl. Acad. Sci. USA **95:**2227–2232.
22. **Janda, M., and P. Ahlquist.** 1993. RNA-dependent replication, transcription, and persistence of brome mosaic virus RNA replicons in *S. cerevisiae*. Cell **72:**961–970.
23. **Kao, C. C., and P. Ahlquist.** 1992. Identification of the domains required for direct interaction of the helicase-like and polymerase-like RNA replication proteins of brome mosaic virus. J. Virol. **66:**7293–7302.
24. **Kong, F., K. Sivakumaran, and C. Kao.** 1999. The N-terminal half of the brome mosaic virus 1a protein has RNA capping-associated activities: specificity for GTP and *S*-adenosylmethionine. Virology **259:**200–210.
25. **Krol, M. A., N. H. Olson, J. Tate, J. E. Johnson, T. S. Baker, and P. Ahlquist.** 1999. RNA-controlled polymorphism in the in vivo assembly of 180-subunit and 120-subunit virions from a single capsid protein. Proc. Natl. Acad. Sci. USA **96:**13650–13655.
26. **Kroner, P. A., B. M. Young, and P. Ahlquist.** 1990. Analysis of the role of brome mosaic virus 1a protein domains in RNA replication, using linker insertion mutagenesis. J. Virol. **64:**6110–6120.
27. **Kujala, P., T. Ahola, N. Ehsani, P. Auvinen, H. Vihinen, and L. Kääriäinen.** 1999. Intracellular distribution of rubella virus nonstructural protein P150. J. Virol. **73:**7805–7811.
28. **Laakkonen, P., T. Ahola, and L. Kääriäinen.** 1996. The effects of palmitoylation on membrane association of Semliki forest virus RNA capping enzyme. J. Biol. Chem. **271:**28567–28571.
29. **Laakkonen, P., M. Hyvönen, J. Peränen, and L. Kääriäinen.** 1994. Expression of Semliki Forest virus nsP1-specific methyltransferase in insect cells and in *Escherichia coli*. J. Virol. **68:**7418–7425.
30. **Laemmli, U. K.** 1970. Cleavage of structural proteins during the assembly of the head of bacteriophage T4. Nature **227:**680–685.
31. **Lampio, A., I. Kilpeläinen, S. Pesonen, K. Karhi, P. Auvinen, P. Somerharju, and L. Kääriäinen.** 2000. Membrane binding mechanism of an RNA virus-capping enzyme. J. Biol. Chem. **275:**37853–37859.
32. **Lee, W. M., M. Ishikawa, and P. Ahlquist.** 2001. Mutation of host Δ9 fatty acid desaturase inhibits brome mosaic virus RNA replication between template recognition and RNA synthesis. J. Virol. **75:**2097–2106.
33. **Molla, A., A. V. Paul, and E. Wimmer.** 1993. Effects of temperature and lipophilic agents on poliovirus formation and RNA synthesis in a cell-free system. J. Virol. **67:**5932–5938.
34. **Noueiry, A. O., J. Chen, and P. Ahlquist.** 2000. A mutant allele of essential, general translation initiation factor DED1 selectively inhibits translation of a viral mRNA. Proc. Natl. Acad. Sci. USA **97:**12985–12990.
35. **O'Reilly, E. K., J. D. Paul, and C. C. Kao.** 1997. Analysis of the interaction of viral RNA replication proteins by using the yeast two-hybrid assay. J. Virol. **71:**7526–7532.
36. **O'Reilly, E. K., N. Tang, P. Ahlquist, and C. C. Kao.** 1995. Biochemical and genetic analyses of the interaction between the helicase-like and polymerase-like proteins of the brome mosaic virus. Virology **214:**59–71.
37. **O'Reilly, E. K., Z. Wang, R. French, and C. C. Kao.** 1998. Interactions between the structural domains of the RNA replication proteins of plant-infecting RNA viruses. J. Virol. **72:**7160–7169.
38. **Pedersen, K. W., Y. van der Meer, N. Roos, and E. J. Snijder.** 1999. Open reading frame 1a-encoded subunits of the arterivirus replicase induce endoplasmic reticulum-derived double-membrane vesicles which carry the viral replication complex. J. Virol. **73:**2016–2026.
39. **Restrepo-Hartwig, M., and P. Ahlquist.** 1999. Brome mosaic virus RNA replication proteins 1a and 2a colocalize and 1a independently localizes on the yeast endoplasmic reticulum. J. Virol. **73:**10303–10309.
40. **Restrepo-Hartwig, M. A., and P. Ahlquist.** 1996. Brome mosaic virus helicase- and polymerase-like proteins colocalize on the endoplasmic reticulum at sites of viral RNA synthesis. J. Virol. **70:**8908–8916.
41. **Rikkonen, M., J. Peranen, and L. Kaariainen.** 1994. ATPase and GTPase activities associated with Semliki Forest virus nonstructural protein nsP2. J. Virol. **68:**5804–5810.
42. **Rose, M. D., L. M. Misra, and J. P. Vogel.** 1989. KAR2, a karyogamy gene, is the yeast homolog of the mammalian BiP/GRP78 gene. Cell **57:**1211–1221.
43. **Russell, P. J., S. J. Hambidge, and K. Kirkegaard.** 1991. Direct introduction and transient expression of capped and non-capped RNA in *Saccharomyces cerevisiae*. Nucleic Acids Res. **19:**4949–4953.
44. **Sambrook, J., E. F. Fritsch, and T. Maniatis.** 1989. Molecular cloning : a laboratory manual, 2nd ed. Cold Spring Harbor Laboratory, Cold Spring Harbor, N.Y.
45. **Schlegel, A., T. H. Giddings, M. S. Ladinsky, and K. Kirkegaard.** 1996. Cellular origin and ultrastructure of membranes induced during poliovirus infection. J. Virol. **70:**6576–6588.
46. **Schröeder, S., F. Schimmöller, B. Singer-Krüger, and H. Riezman.** 1995. The Golgi-localization of yeast Emp47p depends on its di-lysine motif but is not affected by the ret1-1 mutation in alpha-COP. J. Cell Biol. **131:**895–912.
47. **Suhy, D. A., T. H. Giddings, and K. Kirkegaard.** 2000. Remodeling the endoplasmic reticulum by poliovirus infection and by individual viral proteins: an autophagy-like origin for virus-induced vesicles. J. Virol. **74:**8953–8965.
48. **Sullivan, M., and P. Ahlquist.** 1997. *cis*-Acting signals in bromovirus RNA replication and gene expression: networking with viral proteins and host factors. Semin. Virol. **8:**221–230.
49. **Sullivan, M. L., and P. Ahlquist.** 1999. A brome mosaic virus intergenic RNA3 replication signal functions with viral replication protein 1a to dramatically stabilize RNA in vivo. J. Virol. **73:**2622–2632.
50. **Teterina, N. L., K. Bienz, D. Egger, A. E. Gorbalenya, and E. Ehrenfeld.** 1997. Induction of intracellular membrane rearrangements by HAV proteins 2C and 2BC. Virology **237:**66–77.
51. **Teterina, N. L., A. E. Gorbalenya, D. Egger, K. Bienz, and E. Ehrenfeld.** 1997. Poliovirus 2C protein determinants of membrane binding and rearrangements in mammalian cells. J. Virol. **71:**8962–8972.
52. **van der Meer, Y., H. van Tol, J. Krijnse-Locker, and E. J. Snijder.** 1998. ORF1a-encoded replicase subunits are involved in the membrane association of the arterivirus replication complex. J. Virol. **72:**6689–6698.
53. **Wu, S. X., P. Ahlquist, and P. Kaesberg.** 1992. Active complete in vitro replication of nodavirus RNA requires glycerophospholipid. Proc. Natl. Acad. Sci. USA **89:**11136–11140.